A Relaxed Eddy Accumulation System for Measuring Surface Fluxes of Total Gaseous Mercury

JESSE O. BASH* AND DAVID R. MILLER

University of Connecticut, Storrs, Connecticut

(Manuscript received 17 August 2006, in final form 17 May 2007)

ABSTRACT

A relaxed eddy accumulation (REA) system was designed to continuously measure total gaseous mercury (TGM) fluxes over a forest canopy. TGM concentration measurements were measured at 5-min intervals with a Tekran model 2537A mercury analyzer located above the forest canopy on a walk-up meteorological tower. Ten-minute averages for up- and downdraft mercury concentrations were used to calculate the flux. The multiresolution decomposition technique was used to determine day- and nighttime averaging periods for the turbulent statistics used in the REA technique. This paper documents the REA system for mercury flux measurements and its use over a forest canopy.

The REA system response to the averaging times for the turbulent statistics and corrections to up- and downdraft concentrations are major considerations when using the technique with the Tekran mercury analyzer over a forest canopy. TGM flux data collected from 18 August to 12 September 2005 are used here to demonstrate the capabilities of the REA system to measure both short- (1-h time periods) and long-term flux dynamics. During the demonstration period the TGM median flux was 21.9 ± 32.6 ng m^{-2} h^{-1} and the median atmospheric TGM concentrations were 1.34 ± 0.13 ng m^{-2} h^{-1}. Maximum short-term TGM evasive fluxes occurred during the daylight hours with minimums during the nighttime. A consistent bimodal emission pattern was observed during the daytime emissions over the canopy. The first peak occurred immediately following the evaporation of the nighttime dew on the canopy and the second peak occurred in the late afternoon.

1. Introduction

Atmospheric mercury (Hg) loading to fresh- and saltwater bodies has become an important issue since the neurotoxin methylmercury has been found in fish at levels that can pose health risks to some segments of the population (Hammerschmidt and Fitzgerald 2006). To determine the origin of this contamination, it is clear that a better understanding of the mercury cycle is needed. Mercury is a naturally occurring element that cycles between aqueous, terrestrial, and atmospheric systems. Anthropogenic activity has enriched this natural cycle through the combustion of coal and oil for power, the production of chemicals, and the incineration of waste (Pirrone et al. 2001). The contribution of biogenic and physiochemical mercury emissions from land and water surfaces to the total atmospheric mercury load have recently been estimated to be roughly equivalent to anthropogenic emissions (Pirrone et al. 2001; Lindberg et al. 1998). The origins of this spatially distributed Hg at the surface, especially in uncontaminated locations with background soil mercury concentrations, is currently believed to be from wet and dry atmospheric deposition. In this paper we will refer to both natural emissions and reemissions to the atmosphere as "natural emissions." These natural emissions may contribute an estimated 25%–66% of the global mercury emissions budget (Bash et al. 2004; Pirrone et al. 2001; Seigneur et al. 2004). The magnitude and variability of these fluxes to and from the forest canopy and soil surfaces are poorly understood, and previous attempts to measure them are limited spatially and temporally. Little is currently known on the seasonal dynamics of the mercury biogeochemical cycle over this surface due to the lack of published measurements.

* Current affiliation: National Oceanic and Atmospheric Administration/Air Resource Laboratory/Atmospheric Science Modeling Division, in partnership with the National Exposure Research Laboratory, U.S. Environmental Protection Agency, Research Triangle, North Carolina.

Corresponding author address: Jesse Bash, 109 T. W. Alexander Drive, Room D-211E, Research Triangle Park, NC 27711.
E-mail: jesse.bash@noaa.gov

DOI: 10.1175/2007JTECHA908.1

The purpose of this paper is to describe a relaxed eddy accumulation (REA) system designed to measure these total gaseous mercury (TGM) fluxes continuously using 1-h integrations. Example data are presented for measurements over a predominately red maple and white oak closed-canopy forest located at the University of Connecticut (UCONN) experimental farm in Coventry, Connecticut (41°47′30″N, 72°22′29″W).

The REA technique presented here uses the 5-min-average TGM gas concentration measurements from the Tekran model 2537A mercury analyzer. Flux measurements are taken at a single point above the surface of interest, in our case the forest canopy, and are calibrated by accumulating sensible heat flux at that same point.

Only two other attempts have been made to measure TGM fluxes with an REA system. These were made by Cobos et al. (2002) over a cornfield and Olofsson et al. (2005) over an agriculture field. No other measurements of the TGM flux using the REA technique have been made over a forest canopy.

Previous measurements of net mercury fluxes above vegetation

The eddy covariance (EC) technique is often the method of choice for measuring the turbulent flux of gaseous scalars above forest canopies. However, the EC technique requires fast-response measurements (at least 10 Hz) of gas concentration perturbations, and currently no instrument has been devised that can measure ambient TGM concentrations at that frequency. The modified Bowen ratio (MBR) is the only technique that has been used to measure natural TGM fluxes over a forest canopy to date. Dynamic flux chambers (DFCs) have been used to measure fluxes from low vegetation, soil, and individual tree branches, but these measurements are not directly comparable to micrometeorological measurements because of the physical barrier that the chamber imposes (Gillis and Miller 2000; Gustin et al. 2004).

1) THE MBR TECHNIQUE

TGM fluxes over tall canopies were measured by Lindberg et al. (1998) over a forest and by Lee et al. (2000) over a coastal marsh, and reactive gaseous mercury was measured by Lindberg and Stratton (1998) using the MBR technique. The MBR method is a flux–gradient method originally derived from experiments over smooth surfaces (Dyer and Hicks 1970) and later modified to estimate the Bowen ratio directly from the measured gradients (Hicks and Wesely 1978). The MBR technique, following Bowling et al. (2003), is

$$F_{\mathrm{Hg}} = -K\frac{(C_{\mathrm{Hg}})_2 - (C_{\mathrm{Hg}})_1}{z_2 - z_1}, \qquad (1)$$

where F_{Hg} is the TGM flux from the canopy; K is the eddy diffusivity; and $(C_{\mathrm{Hg}})_1$ and $(C_{\mathrm{Hg}})_2$ are the ambient TGM concentrations at the two heights z_1 and z_2, respectively.

In the above relationship, the TGM concentration gradient is measured either by gold trap sampling (Lindberg et al. 1998) or, more recently, with a Tekran mercury gas analyzer (Lee et al. 2000; Lindberg et al. 2002). An eddy exchange coefficient (K_H) is calculated for sensible heat flux using a fast-response eddy covariance heat flux measurement from a collocated sonic anemometer, and a simultaneous temperature profile from collocated temperature sensors. In Eq. (1), K_{Hg} for Hg is then estimated from K_H using similarity arguments.

The MBR technique is poorly suited for flux measurements above forests. This technique depends on an accurate measure of time-averaged, very small, concentration gradients, which can be adversely affected by site location and variations in turbulent intensity above the forest (Lindberg et al. 1998). During convective periods the very high-turbulence environment is dominated by large-canopy-scale eddies above the rough canopy. To capture the resultant fluxes requires measurements of gradients over very large vertical distances ($>0.5h$, where h is the canopy height) to obtain the well-defined profiles needed for the MBR technique. In the roughness sublayer, below $1.5h$, the flow and gradients are greatly influenced by air dynamics and thermal effects attributed to the rough surface of a forest canopy (Raupach 1979). The MBR flux measurements have the added complexity of simultaneously measuring the gradient and flux of a trace scalar (generally temperature and sensible heat flux), as well as the Hg concentration gradient (Cobos et al. 2002).

2) THE REA TECHNIQUE

REA techniques, developed originally to measure carbon dioxide (CO_2), water vapor, and sensible heat fluxes (Desjardins 1972), have been successfully used to measure a number of trace gas fluxes. These include volatile organic vapor fluxes above forests (Bowling et al. 1998; Pattey et al. 1999) and a golf course (Olofsson et al. 2003), ammonia volatilization over an agricultural field (Zhu et al. 2000), stable isotope fluxes of $^{13}C^{16}O_2$ and $^{12}C^{18}O^{16}O$ (Bowling et al. 1999), and nitrous oxide (N_2O) fluxes from agricultural land (Xi et al. 1996). Only Cobos et al. (2002) and Olofsson et al. (2005) have reported REA measurements of TGM fluxes. Cobos et al. (2002) made measurements in Minnesota over a

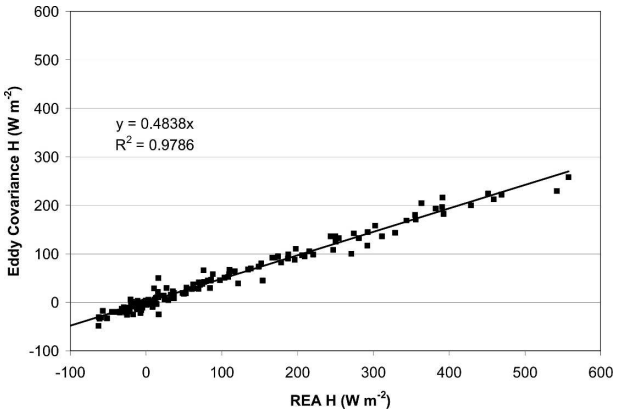

FIG. 1. Scatterplot of the eddy covariance sensible heat fluxes and the simultaneous relaxed eddy accumulation sensible heat fluxes.

cornfield for approximately 2 weeks, and Olofsson et al. (2005) made measurements in Sweden over a contaminated agricultural field.

The REA technique combines fast-response vertical anemometry to detect upward and downward air motions, with a fast-response inlet valve to isolate the air of updrafts from the air of downdrafts. The scalar material carried in the isolated upward- and downward-moving air is then accumulated into separate reservoirs or sampled from the isolated lines. The scalar concentrations are measured with the available slow-response instrumentation, in this case a Tekran model 2537A mercury vapor analyzer. Flux is calculated following Businger and Oncley (1990):

$$F_{\mathrm{TGM}} = \beta\sigma_w(C^+_{\mathrm{TGM}} - C^-_{\mathrm{TGM}}), \qquad (2)$$

where the TGM flux F_{TGM} (ng m^{-2} h^{-1}) is the product of the TGM concentration difference in the up- and downdrafts, C^+_{TGM} (ng m^{-3}) and C^-_{TGM} (ng m^{-3}), respectively. Here, σ_w (m h^{-1}) is the standard deviation of the vertical wind speed and β (unitless) is the relaxation coefficient. The relaxation coefficient is calculated by accumulating the sonic temperature from the sonic anemometer to determine an eddy accumulation measurement of the sensible heat flux without the relaxation coefficient (EA_H), where $\mathrm{EA}_H = \sigma_w(\mathrm{Ts}^+ - \mathrm{Ts}^-)$. Then EA_H is linearly correlated with the simultaneous eddy covariance heat flux (EC_H), where $\mathrm{EC} = \overline{w'\mathrm{Ts}'}$, as demonstrated in Fig. 1. The slope of this line ($\mathrm{EC_H/EA_H}$) is then taken as β, and the assumed similarity between the sensible heat and TGM fluxes is used to apply β to the TGM flux (Cobos et al. 2002; Businger and Oncley 1990).

A vertical wind speed dead band has been show to increase the difference between up- and downdraft concentrations in previous systems (Bowling et al. 1999). However, the REA system described in this paper was developed for reliable seasonal measurements of the TGM flux over a forest canopy. Therefore, a single-inlet REA system was chosen for simplicity and reliability. The Tekran model 2537A mercury analyzer requires a constant airflow for gaseous TGM measurements. To introduce a dead band, a two-inlet REA system would have to be developed and the up- and downdrafts would have to be further diluted with mercury-free air during periods when the vertical wind speed was at a magnitude below the dead band. The concentration differences between the up- and downdrafts may be increased, but the uncertainty in the mercury concentration measurement would have been decreased due to the smaller volume of up- and downdrafts sampled. The addition of more solenoid values and the additional tubing required for a two-inlet REA system would have introduced additional points of potential equipment failure and contamination.

2. Methods

University of Connecticut TGM REA system description

The UCONN single-inlet REA system for measurement of the atmosphere–surface TGM flux is diagramed in Fig. 2. The system is similar to the Cobos et al. (2002) approach, but is modified as suggested by Bowling et al. (1998) to eliminate negative pressure that builds up behind the sampling valve (valve a in Fig.

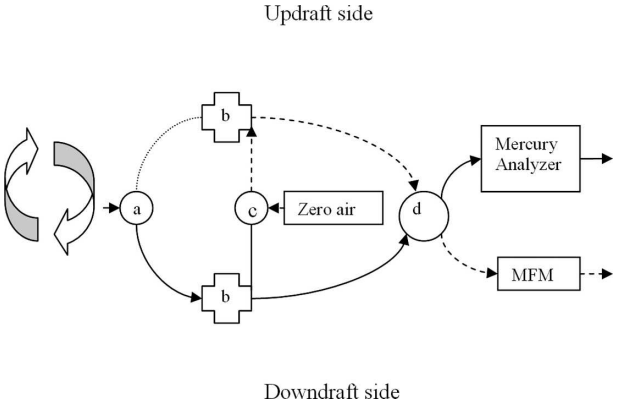

FIG. 2. A diagram of the REA system, where arrows indicate the direction of the airflow during a downdraft when the mercury analyzer is measuring the downdraft samples: (a) three-way inlet valve, (b) particulate filters, (c) three-way zero mercury concentration air valve, and (d) four-way valve to direct up- and downdrafts to the mercury analyzer, where MFM is a digital mass flowmeter. Black solid arrows indicate downdrafts and black dashed arrows indicate updrafts.

TABLE 1. REA components.

Component	Manufacturer	Model number
Mercury analyzer	Tekran	2537A
Flow controller	Tylan General	FC 280
Datalogger	Campbell Scientific	CR5000
Anemometer	Campbell Scientific	CSAT3
Krypton hygrometer	Campbell Scientific	KH2O
Temperature/RH probe	Campbell Scientific	CR500
Teflon tubing	Nalgene	¼ O.D.
Pyrometer	Licor	LI190
Three-way Teflon valve	NResearch	648T031
Two-way Teflon valve	NResearch	648T021
Rain gauge	Capmbell Scientific	TE525
Leaf wetness sensor	Campbell Scientific	CS237

2). TGM concentrations are measured using a Tekran model 2537A cold vapor fluorescent spectrometer mercury gas analyzer. The system differs from that of Olofsson et al. (2005) by using a single Hg analyzer rather that separate analyzers for the up- and downdraft concentrations.

Table 1 is a complete list of the REA system components. The sensors and system switching are controlled and recorded with the Campbell Scientific, Inc., CR5000 datalogger. The datalogger program is available from the authors.

The REA system operates in the following sequence:

1) The sonic anemometer measures the magnitude of the vertical wind.
2) The vertical wind speed signal is sent to the Campbell Scientific, Inc., CR5000 datalogger.
3) The CR5000 datalogger responds by relaying a voltage signal to the sampling valve a, depending on the sign of the vertical wind component.
4) The valve either opens or closes in response to the voltage from the CR5000 to let the up-/downdraft air into either the updraft or downdraft stream of air. Valve c opens or closes to mix clean air into the opposite stream from the sampling valve.
5) The air in the up- and downdraft streams are sampled for gaseous mercury for 10-min intervals before the four-way valve (valve d) switches the sample streams.

The time it takes the air to travel the length of the intake tubing to the sampling valve is matched to the two-scan time delay that is necessary to relay the vertical wind speed information from the CSAT3 to the CR5000 datalogger and then activate the sampling valve.

A constant flow rate and constant density of air is maintained through the use of a second high-speed valve (valve c), following Bowling et al. (1998), to introduce dry, zero mercury concentration air into the stream that is closed at valve a. The modification introduces mercury-free clean air at valve c in Fig. 2. Thus, the Tekran mercury analyzer measures air from one sample line for the sampling period mixed with mercury-free air from valve c. The true up- and downdraft concentrations are calculated by dividing the measured concentration by the ratio of the time of up- and downdrafts to the total sampling time, as follows:

$$C_{\mathrm{Hg}}^{+} = \frac{m_{\mathrm{Hg}}^{+}}{Q\delta t}\frac{\delta t}{\delta t^{+}}$$
$$C_{\mathrm{Hg}}^{-} = \frac{m_{\mathrm{Hg}}^{-}}{Q\delta t}\frac{\delta t}{\delta t^{-}}, \qquad (3)$$

where m_{Hg}^{+} and m_{Hg}^{-} are the mass (ng) of TGM collected on the mercury analyzer's gold traps for up- and downdraft sampling, respectively; Q is the flow rate ($\mathrm{m^3\ s^{-1}}$) through the gold traps during sampling; δt is the duration (s) of the sampling period; and δt^{+} and δt^{-} are the duration (s) of up- and downdrafts during the sampling of the up- and downdrafts, respectively.

The mercury analyzer makes two, 5-min measurements of the same up- or downdraft stream before valve d switches to the other sample stream. The two columns in the Tekran are sampled for 5 min each and then averaged. This eliminates biases in the flux due to differences that may exist between the two Tekran 2537A CVAFS mercury analyzer's gold trap cartridges. TGM concentrations are then saved on a computer and the fast-response turbulence data and statistics are logged on the CR5000 datalogger.

The REA system utilizes NResearch, Inc., model 648T031 three-way polytetrafluoroethylene (PTFE)-bodied isolation valves capable of operating at a maximum switching speed of 10 Hz. One is at the sampling inlet and one is at valve c to sample up- and downdrafts separately and to release zero air into the closed line.

Two high-precision mass flow controllers are used to maintain the consistent flow rate required for the REA technique. A Tylan General FC 280 is located in the mercury analyzer, and an identical mass flow controller is located downstream on the other exhaust of the REA system. Both mass flow controllers maintain a flow rate of 1.5 L $\mathrm{min^{-1}}$. They regulate the flow by measuring heat transfer in the boundary layer, or near the wall, of a heated tube; thus, no density corrections are needed for temperature variations in up- and downdrafts, but corrections are needed for variations in the water vapor content of the air (Webb et al. 1980; Pattey et al. 1992;

Lee 2000). These were made for water vapor following Lee (2000):

$$f_{\mathrm{Hg}} = (1 + 1.85r)F_{\mathrm{Hg}} + 1.85S_{\mathrm{Hg}}E, \quad (4)$$

where f_{Hg} is the density-corrected TGM flux (ng m^{-2} h^{-1}), F_{Hg} is the uncorrected TGM flux (ng m^{-2} h^{-1}) from Eq. (2), E is the water vapor flux (ng m^{-2} h^{-1}), S_{Hg} is the ambient TGM vapor mixing ratio, and r is the water vapor mixing ratio.

3. Results

a. Performance of the REA system

1) Effects of the pressure control system

Initially, the REA system was tested and calibrated over a turf field without the use of the zero air line. No irregularities were noticed in the flow rate at the sampling tube when the system was located over this relatively smooth surface. But, once the system was mounted on the tower over the very rough forest canopy, variability in the flow rate was noted in the output of the Tylan General mass flow controllers located in Tekran mercury analyzer and upstream from the REA exhaust pump (Fig. 2). The variability in the flow rate was then independently confirmed with a DryCal ML-500 high-precision, ±0.25% volumetric flow rate, primary piston mass flowmeter by placing it in series with the sample inlet and also in series with the REA system exhaust.

This variability was caused by a vacuum created behind the sampling valve during periods of low eddy turnover. The eddy turnover frequency above the forest canopy was approximately 1 Hz during unstable conditions and periods of moderate to high wind speed. The eddy turnover frequency above the grass was at least 3 times as fast as that over the forest, and therefore the variability in the flow rate was much smaller. The original TGM REA flux system design developed by Cobos et al. (2002) was then modified by adding a clean air inlet following Bowling et al. (1998) (valve c in Fig. 2). This maintained a consistent flow rate through the sampling tube and eliminated the problem. The inconsistencies in the flow rate through the mercury analyzer, which are a function of the turbulence scale and underlying surface characteristics, are a subtle but important problem, which makes it difficult to transfer REA systems that are designed for smooth surfaces and low vegetation for use over forests. Before the introduction of the clean air line in the REA system over the forest canopy, the flow rate through the mercury analyzer fluctuated as much as ±50% of the magnitude of the expected flow rate. The introduction of the clean air inlet reduced the fluctuation in the flow rate to less than ±0.1% of the magnitude of the desired rate.

2) Limitation of the REA technique during precipitation

The REA technique relies on an open-path sonic anemometer. When the sending head or the receiving heads become wet, the sensors do not function properly. The data were sanitized using the error signals sent from the CSAT3 sonic anemometer. Measurements were rejected when the error in the instrument accounted for 0.5% or more of the measurements in the averaging window. Over a year's period in subhumid Connecticut, rain events resulted in a 13% loss of data.

3) Averaging time for REA fluxes

Both the REA and EC techniques are derived from the flow equations using Reynolds averaging (Stull 1988; Businger and Oncley 1990) and assume that the averaging length of the time series includes the entire turbulent signal (Stull 1988). We determine the averaging times for the turbulent statistics, σ_w [Eq. (2)] and eddy covariance fluxes, in the REA system using multiresolution decomposition (MRD) analyses after Howell and Mahrt (1997) and Vickers and Mahrt (2003). Hourly averages of the turbulent statistics calculated on the MRD time scale are used for the hourly TGM flux calculations. The MRD spectra are used much like a Fourier spectral analysis to determine the spectral gap between fluxes on the turbulent time scale and fluxes on mesoscale or synoptic fluxes. However, the MRD spectra do not assume periodicity or a stationary time series (Howell and Mahrt 1997). This helps improve the similarity relationships between scalars essential to the EC and REA techniques. Multiresolution spectra and cospectra are calculated following Howell and Mahrt (1997):

$$D_w(2^m) = \frac{1}{2^M}\sum_{i=0}^{2^M-1}[w_i - \overline{w}(2^m)]^2,$$

$$D_{w\phi}(2^m) = \frac{1}{2^M}\sum_{i=0}^{2^M-1}[w_i - \overline{w}(2^m)][\phi_i - \overline{\phi}(2^m)], \quad (5)$$

where D_w and $D_{w\varphi}$ are the multiresolution spectra and cospectra, respectively; 2^m is the length of the averaging window used to calculate the geometric means $\overline{w}$ and $\overline{\phi}$; and 2^M is the length of the data series. This averaging time is then binned into its nearest increment divisible by 5 min in order to match the output time for each sample of the mercury analyzer; once an appropriate

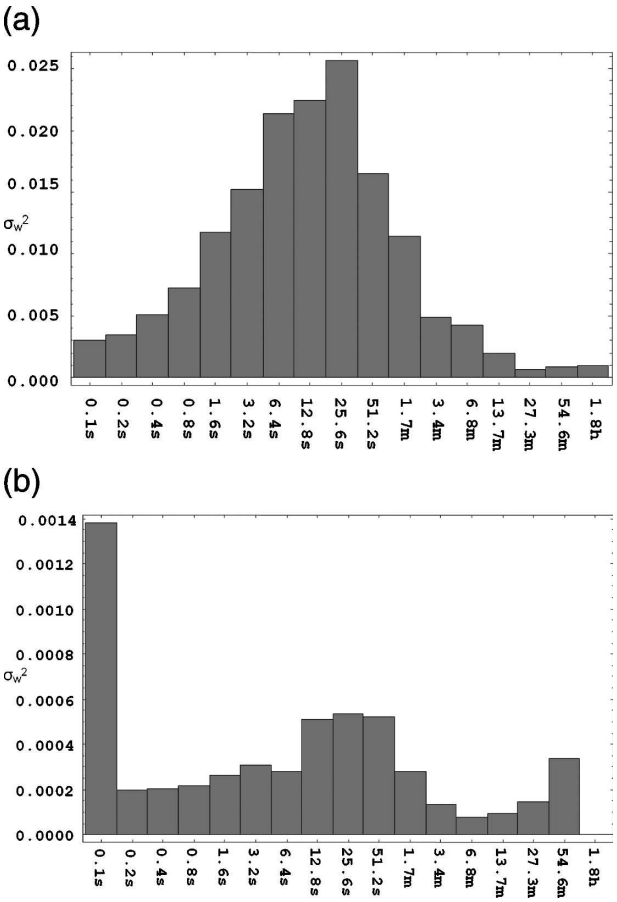

FIG. 3. Mutiresolution orthogonal decomposition of the vertical wind speed under (a) unstable daytime and (b) stable nighttime conditions on 30 Jul 2004.

averaging time has been established, micrometeorological parameters and fluxes can be calculated using Reynolds averaging (Stull 1988).

The spectral gaps calculated using the MRD technique were located between 15 and 60 min for convective daytime conditions (Fig. 3a), and the spectral gap ranged from 5 to 10 min during periods of strong nighttime stability over the forest canopy (Fig. 3b). The 5-min averaging period used by the Tekran mercury analyzer and the hourly averaging period used in flux calculations included more vertical wind speed variability than using the averaging period determined using the MRD technique. Thus, a 30-min averaging period was used for the calculations of the turbulent statistics used in both the EC and REA systems for daytime periods, from an hour after sunrise to an hour before sunset, and a 10-min averaging period was used during the night. This averaging scheme calculated the turbulent statistics on a time scale that agreed with the results from MRD spectra for most day- and nighttime conditions.

Note that the averaging times for the turbulent statistics, that is, σ_w, determined above, are not the same as the accumulation times for the ratios $\delta t/\delta t^+$ and $\delta t/\delta t^-$ in Eq. (3), which are used to correct the TGM concentrations diluted by the clean air inlet. Three scenarios, shown in Table 2, demonstrate the time dependence of the up- and downdraft time ratios and the corrected TGM concentration. The first scenario measured the up- and downdraft ratios for the entire hour, the second measured the ratios during the 10-min up- and downdraft sampling periods, and the third measured the up- and downdraft ratios for each 5-min sampling period of the mercury analyzer. The long time periods of 1 h introduced oscillations into the calculated fluxes as demonstrated in Fig. 4. The 5- and 10-min scenarios generally agreed with each other much better, but there were instances where the 10-min scenario under- or overpredicted the flux (Fig. 4). We recommend using up- and downdraft time ratio averaging periods that are equal to the sampling period of the analyzer used in the REA system.

The Tekran 2537A mercury analyzer was calibrated in situ on approximately a weekly basis using the internal permeation sources and a mercury-free zero air source. In May 2004 and January 2005, the Tekran 2537A mercury analyzer was shipped to the Tekran laboratory in Toronto, Ontario, Canada, for repairs, upgrades, and calibrations. Calibrations in the field were preformed after interruptions of the mercury analyzer's power due to inclement weather, and when trends in the TGM concentration or fluxes were observed. In all cases, a successful calibration did not effect the TGM concentration or the magnitude or direction of the TGM flux as demonstrated in Fig. 5.

TABLE 2. Up- and downdraft averaging schemes used to correct the measured mercury flux according to Eq. (3). Lightface text and + indicate updrafts and bolded text and − indicate downdrafts.

Time	5	10	**15**	**20**	25	30	**35**	**40**	45	50	**55**	**60**
Cartridge	A+	B+	**A−**	**B−**	A+	B+	**A−**	**B−**	A+	B+	**A−**	**B−**
Up- and downdraft averaging schemes	Full hour up- and downdraft time ratios											
	+		−		+		−		+		−	
	+	+	−	−	+	+	−	−	+	+	−	−

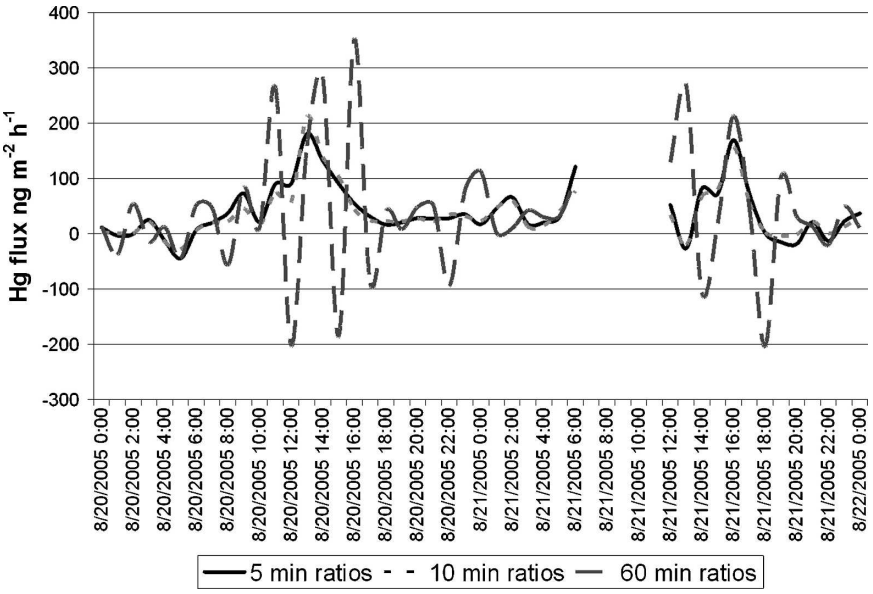

FIG. 4. TGM flux calculated using 5-, 10-, and 60-min average up- and downdraft ratios from 20 Aug 2005 through 21 Aug 2005.

4) FOOTPRINT ANALYSIS OF THE MEASUREMENT SITE

An Eulerian analytic flux footprint model following Amiro (1998) was implemented for the tower site to estimate the probable source areas contributing to the fluxes measured. The footprint was calculated as follows:

$$F(x, y, z) = f'(x, z)D_y(x, y), \tag{6}$$

where $F(x, y, z)$ is the flux footprint (m^{-2}), x is the streamwise distance, y is the lateral distance, and z is the centerline vertical distance. Here $f(x, z)$ is the crosswind footprint [m^{-1}; Eq. (2)] and $D_y(x, y)$ is the Gaussian dispersion (m^{-1}) in the lateral direction.

The crosswind-integrated footprint model was developed by Amiro (1998) and is based on a gradient-diffusion model as follows:

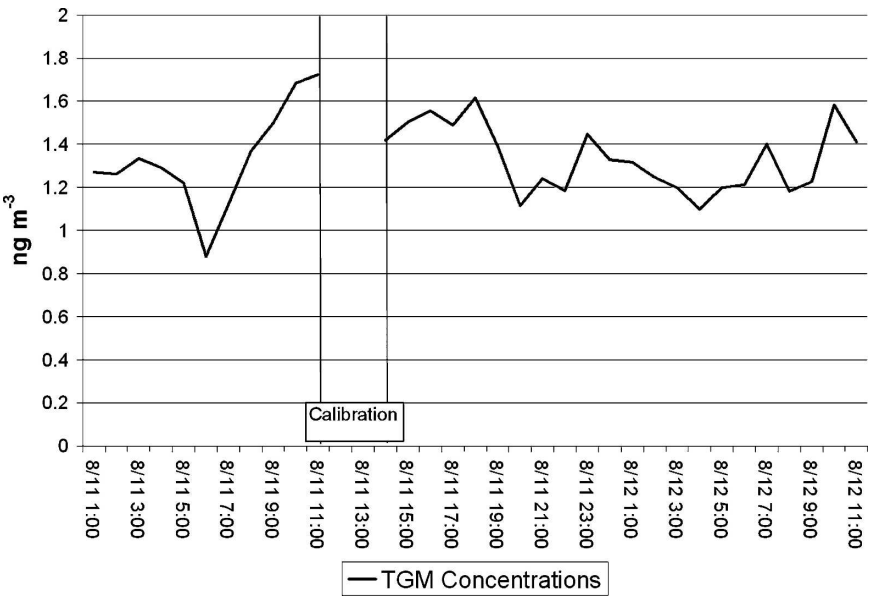

FIG. 5. TGM concentrations before a calibration on 11 Aug and after the calibration.

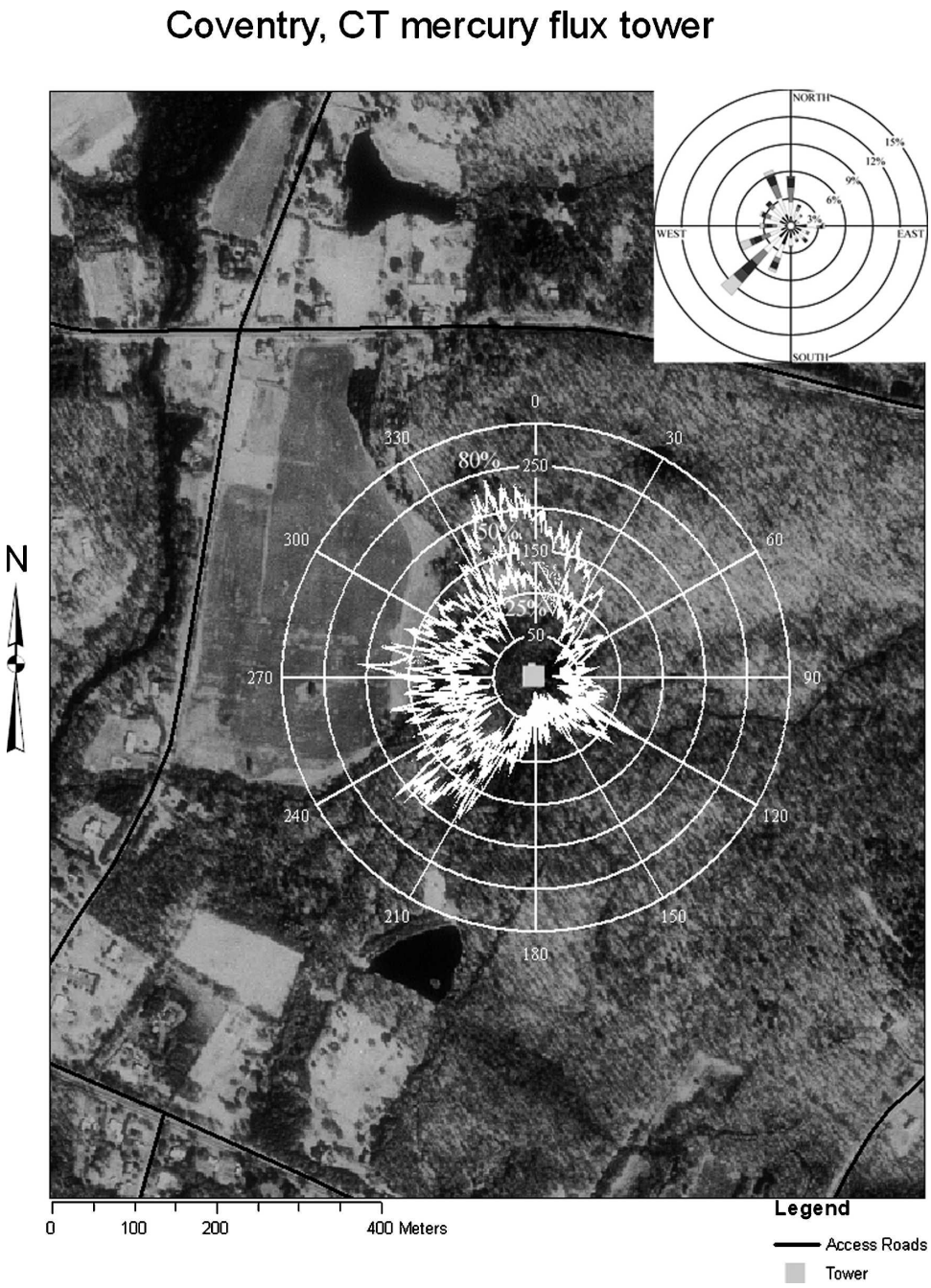

FIG. 6. Contours containing 80%, 50%, and 25% of the flux and a wind rose during unstable conditions at the measurement site.

$$f'(x, z) = \left(\frac{\Phi}{z_m}\right)\left\{\frac{k^2}{\phi_m\left[\ln\left(\frac{pz}{z_o}\right) - \psi\right]}\right\}, \quad (7)$$

where Φ is the normalized crosswind-integrated footprint, z_m is the measurement height, and k is the von Kármán constant (0.4). The dimensionless wind shear ϕ_m and the diabatic correction factor ψ are calculated following Stull (1988). The normalized crosswind-integrated footprint is calculated following Horst and Weil (1994):

$$\Phi = \left(\frac{z_m}{z}\right)\frac{\overline{u}(z_m)}{\overline{U}(z)} A \exp\left[-\left(\frac{z_m}{bz}\right)^r\right], \quad (8)$$

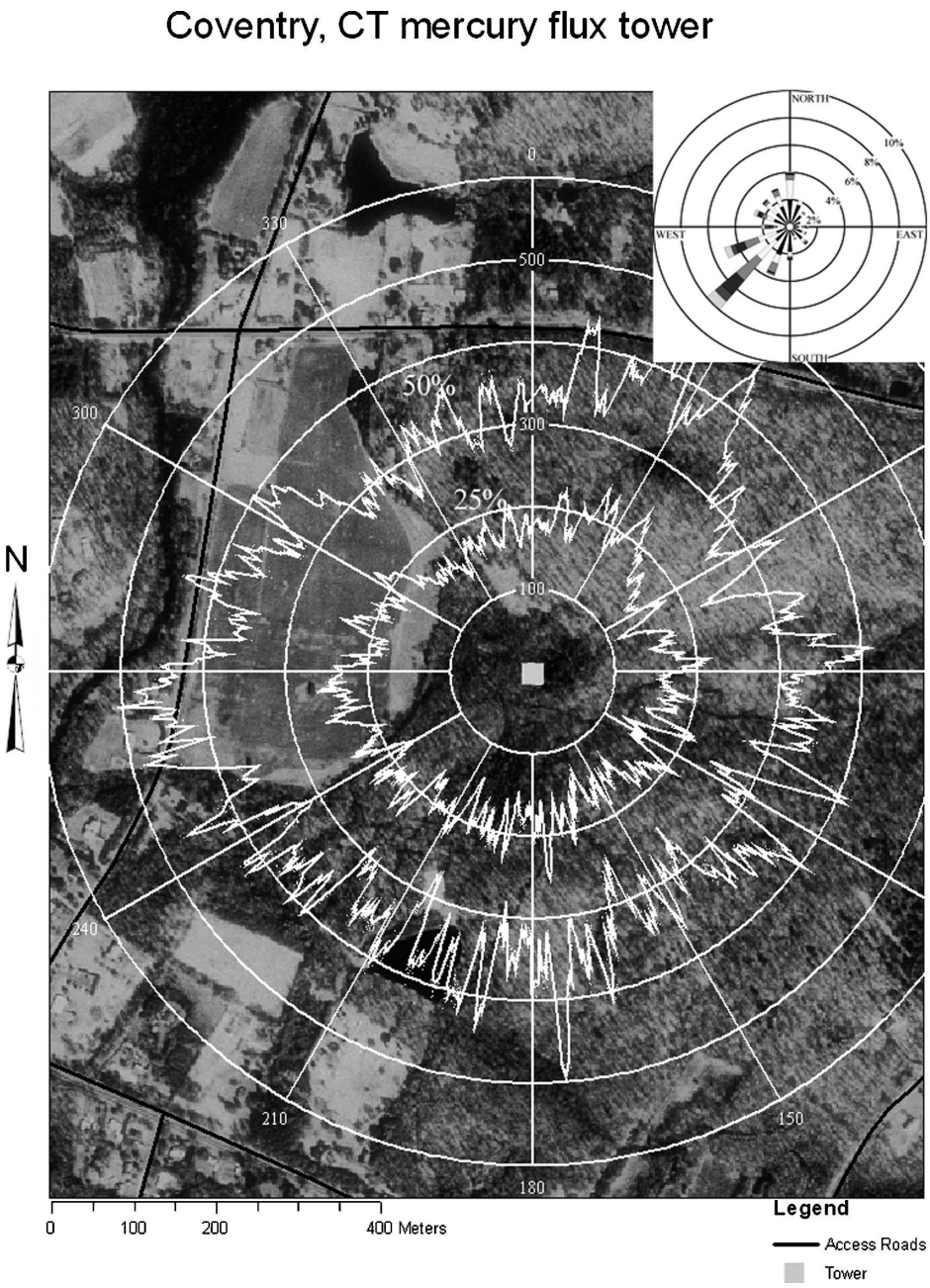

FIG. 7. Contours containing 50% and 25% of the flux and a wind rose during stable conditions at the measurement site.

where $\overline{u}(z_m)$ is the wind speed at the height of the measurements and $\overline{U}(z)$ is the effective speed of wind advection; *A, b,* and *r* are calculated using gamma functions following Gryning et al. (1983).

The footprint model was calculated using a year of meteorological data collected in 2004 at the flux tower site. Contour maps were then compiled using the cross-wind-integrated footprint for unstable ($z/L < 0$) and stable ($z/L > 0$) conditions (see Figs. 7 and 8). During unstable conditions the prevailing wind directions were from the southwest and north-northwest (Fig. 6). The majority of the flux was estimated to originate from areas within the forest for all wind directions, except from approximately due west.

Under stable conditions the distance to 80%, 50%, and 25% flux contours increased greatly, as shown in Fig. 7. Less than half of the flux was estimated to originate from the forest for wind blowing from the west.

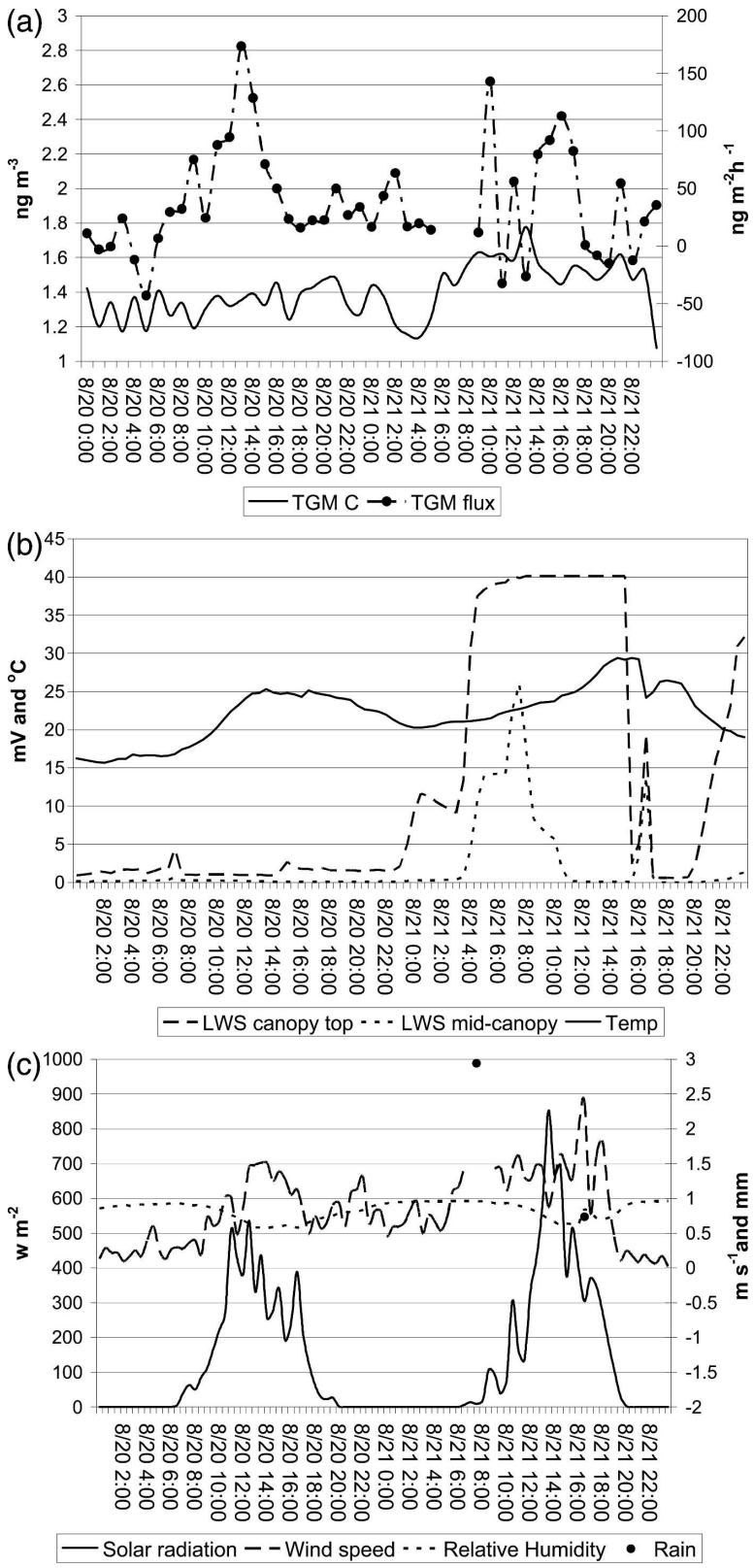

FIG. 8. (a) The TGM flux and ambient TGM concentration; (b) leaf wetness sensors (LWS) at the top and midcanopy and temperature; and (c) incoming solar radiation, wind speed, and rainfall from 20 to 22 Aug 2005.

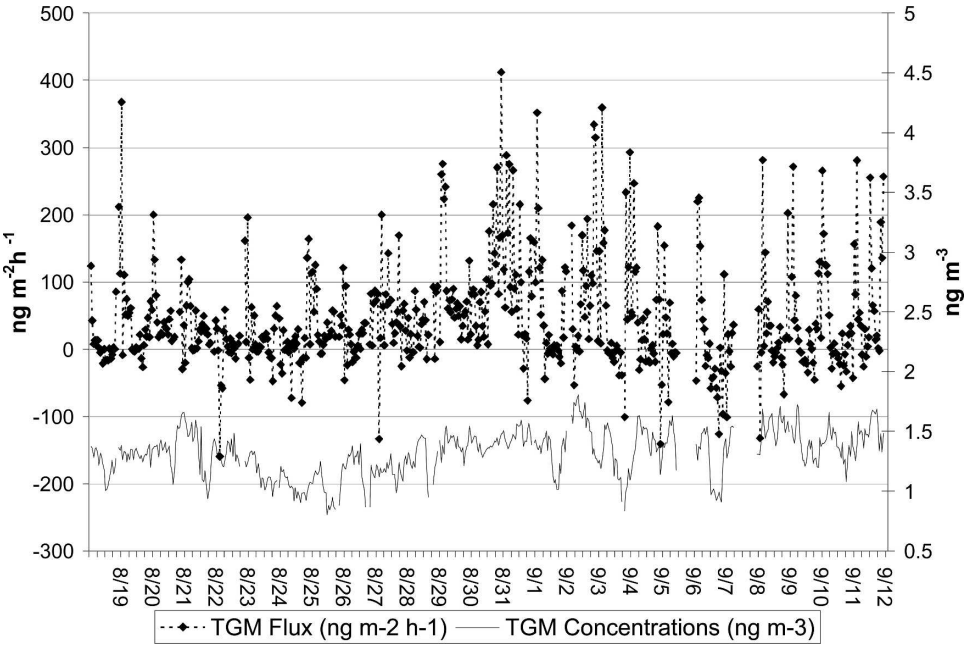

FIG. 9. TGM flux and concentration measurements from 18 Aug to 12 Sep 2005.

However, the prevailing wind direction was from the southwest, which is an area of relatively good fetch. Fluxes are generally small under stable conditions due to the low vertical mixing of air parcels.

We use the above footprint analysis to asses the quality of the fluxes measured, filter the data from periods when the flux is predicted to originate from area of poor fetch, and identify the local origins of evasion.

b. TGM flux measurements

The REA system was mounted on a walkup tower at approximately 1.3h (h = canopy height) in the 20-m-tall forest. At this height in the forest canopy roughness sublayer, the air is generally mixed enough to characterize the forest canopy but is still close enough to the forest canopy to minimize the fetch inhomogeneities.

A 2-day time series from 20 through 21 August is shown in Figs. 8a–c. There was a light drizzle in the morning of 20 August that did not register on the rain gauge but was observed with the leaf wetness sensors (Fig. 8b). Figure 8a shows that the atmospheric TGM concentration was around 1.5 ng m^{-3} on 20 August, rose slightly to approximately 1.7 ng m^{-3} on 21 August, and fell to 1.3 ng m^{-3} after a weak cold front had passed. The TGM evasive flux was highest during 20 August, which was a dry but cloudy day. Heavy rain fell from 0700 to 0830 LT and again at 1630 LT 21 August, with the passage of the cold front. Wet sensors made the data suspect after the morning rain, but strong emissions of TGM were observed following the afternoon precipitation event on 21 August. Evasion from the forest canopy peaked when the leaf wetness sensors indicated that the midcanopy had dried. This can be interpreted either as a stomatal control of the TGM flux, as in Lindberg et al. (1998), or as evasion of mercury deposited via wet deposition, as documented by Graydon et al. (2006).

Hourly data from 18 August to 12 September 2005 are shown in Fig. 9. The data collected over this period were skewed to the right due to several evasion events—one following a light rain storm, with a total precipitation of 10 mm, lasting from 30 August to 1 September. The median was used as the measure of central tendency, and median absolute deviation (MAD) was used as the measure of scatter because both methods are not as sensitive to the tails of the distribution as the mean and standard deviation (Wilks 1995). The net TGM flux was positive with a median TGM flux of 21.9 ± 32.6 ng m^{-2} h^{-1} (with a mean of 44.4 ng m^{-2} h^{-1} and a standard deviation of 78.8 ng m^{-2} h^{-1}) and the median TGM concentrations were 1.34 ± 0.13 ng m^{-3} (with a mean of 1.32 ng m^{-3} and a standard deviation of 0.19 ng m^{-3}). Lindberg et al. (1998) and Lee et al. (2000) described the only other mercury flux campaigns that measured TGM fluxes over tall canopies using micrometeorological techniques. The diurnal pattern and magnitude shown here are lower than the fluxes from the Lindberg et al.

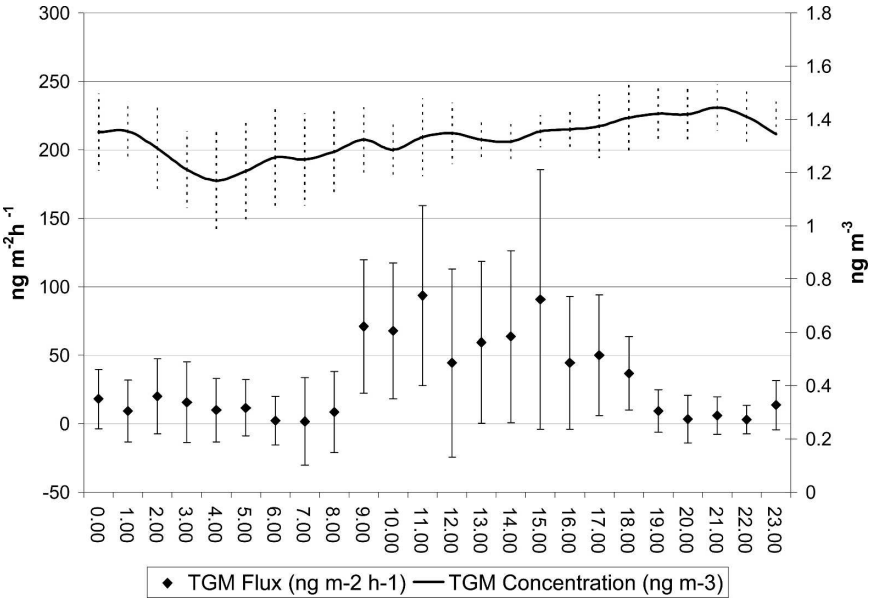

FIG. 10. The median daily TGM fluxes and atmospheric concentrations from 18 Aug 2005 to 12 Sep 2005. The error bars represent one median absolute deviation.

(1998) unfiltered data over a hardwood canopy (~100 ± 80 ng m^{-2} h^{-1}) and are similar to their results from large gradient measurements in a Tennessee pine plantation (43 ± 29 ng m^{-2} h^{-1}). Lee et al. (2000) reported deposition to a tall canopy over a coastal salt marsh during the spring and early summer of 1997 and 1998, with the maximum deposition occurring during daytime hours. The measurements presented here were taken during the mid- to late summer; however, springtime measurements at the site exhibited deposition with the maximum during the day consistent with that of Lee et al. (2000) and Bash and Miller (2007, manuscript submitted to *Appl. Geochem.*). The maximum TGM evasive flux occurred during the daylight hours, with the

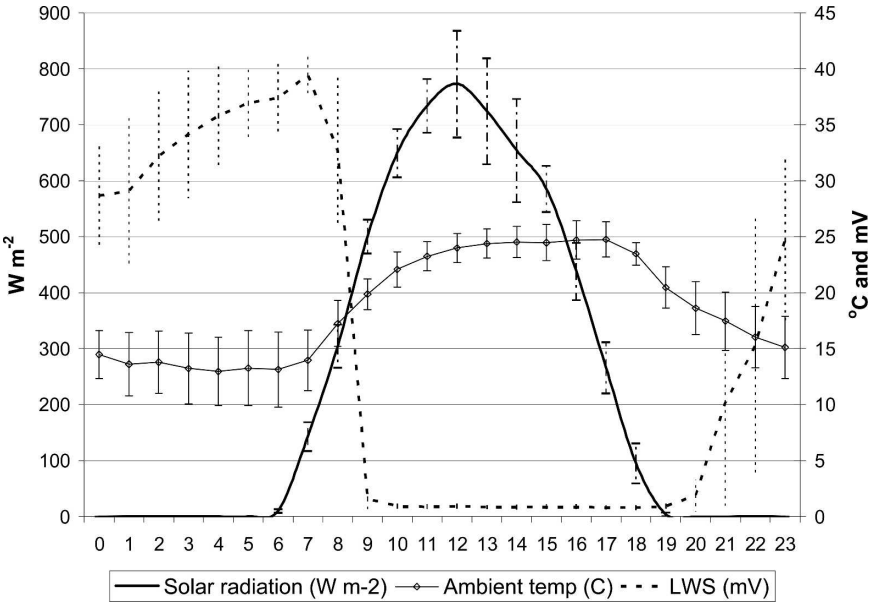

FIG. 11. The median daily incoming solar radiation, ambient temperature, and leaf wetness sensor voltage output from 18 Aug 2005 to 12 Sep 2005. The error bars represent one median absolute deviation.

minimum during the nighttime (Figs. 9 and 10). A consistent bimodal emission pattern was observed during the daytime emissions over the canopy (Fig. 10). The first peak appears to be from canopy TGM emissions immediately following the evaporation of the nighttime dew on the canopy (Figs. 10 and 11), in agreement with Lindberg et al. (1998). The second peak occurs during the late afternoon just after the peak incoming solar radiation and just before the afternoon high temperature (Figs. 10 and 11).

4. Summary

The relaxed eddy accumulation technique eliminates many, but not all, of the flux–gradient problems for TGM flux measurements above rough surfaces. The REA technique separates the air at a single point above the surface into updrafts and downdrafts. Fluxes are then calculated by measuring the average concentration of TGM in the air in the updrafts and the average concentration of TGM in the air in the downdrafts.

The system presented here measures TGM concentrations with a Tekran model 2537A cold vapor florescent spectrometer that requires airflow for 5 min to acquire a single sample. The REA system utilizes a single inlet and separates the air from it into an updraft line and a downdraft line. It includes a clean air inlet, after Bowling et al. (1998), to offset vacuum buildup behind the sampling valve in the nonsampling line. The use of a single Tekran model 2537A mercury analyzer allowed the system to be automated and avoided the potential biases between two mercury analyzers, as used in the system developed by Olofsson et al. (2005). Averaging periods for the turbulent statistic σ_w are determined by multiresolution decomposition after Vickers and Mahrt (2003). Density corrections for TGM and water vapor are made to the flux calculations.

The results obtained using the REA technique for mercury flux measurements over a forest canopy are comparable to those obtained by Lindberg et al. (1998).

Acknowledgments. We thank the helpful comments of two anonymous reviewers. This research was funded by the Connecticut River Basin Airshed–Watershed Consortium and the University of Connecticut, College of Agriculture, Storrs Agricultural Experiment Station. Special thanks to Dr. Xuhui Lee, of Yale University, for his suggestions and ideas on the manuscript and density corrections for the REA system.

REFERENCES

Amiro, B. D., 1998: Footprint climatologies for evapotranspiration in a boreal catchment. *Agric. For. Meteor.,* **90,** 195–201.

Bash, J. O., D. R. Miller, T. H. Meyer, and P. A. Bresnahan, 2004: Northeast United States and Southeast Canada natural mercury emissions estimated with a surface emission model. *Atmos. Environ.,* **38,** 5683–5692.

Bowling, D. R., A. A. Turnipseed, A. C. Delany, D. D. Baldocchi, J. P. Greenberg, and R. K. Monson, 1998: The use of relaxed eddy accumulation to measure biosphere-atmosphere exchange of isoprene and other biological trace gases. *Oecologia,* **116,** 306–315.

——, A. C. Delany, A. A. Turnipseed, D. D. Baldocchi, and R. K. Monson, 1999: Modification of the relaxed eddy accumulation technique to maximize measured scalar mixing ratio differences in updrafts and downdrafts. *J. Geophys. Res.,* **104** (D8), 9121–9133.

——, D. E. Pataki, and J. R. Ehleringer, 2003: Critical evaluation of micrometeorological methods for measuring ecosystem–atmospheric isotopic exchange of CO_2. *Agric. For. Meteor.,* **116,** 159–179.

Businger, J. A., and S. P. Oncley, 1990: Flux measurement with conditional sampling. *J. Atmos. Oceanic Technol.,* **7,** 349–352.

Cobos, D. R., J. M. Baker, and E. A. Nater, 2002: Conditional sampling for measuring mercury vapor fluxes. *Atmos. Environ.,* **36,** 4309–4321.

Desjardins, R. L., 1972: A study of carbon-dioxide and sensible heat fluxes using the eddy correlation technique. Ph.D. dissertation, Cornell University, 189 pp.

Dyer, A. J., and B. B. Hicks, 1970: Flux gradient relationships in the constant flux layer. *Quart. J. Roy. Meteor. Soc.,* **96,** 715–721.

Gillis, A., and D. R. Miller, 2000: Some potential errors in the measurement of mercury gas exchange at the soil surface using a dynamic flux chamber. *Sci. Total Environ.,* **260,** 181–189.

Graydon, J. A., V. L. St. Louis, S. E. Lindberg, H. Hintelmann, and D. P. Krabbenhoft, 2006: Investigation of mercury exchange between forest canopy vegetation and the atmosphere using a new dynamic chamber. *Environ. Sci. Technol.,* **40,** 4680–4688.

Gryning, S.-E., A. P. Ulden, and S. E. Larsen, 1983: Dispersion from a continuous ground-level source investigated by a *K* model. *Quart. J. Roy. Meteor. Soc.,* **109,** 355–364.

Gustin, M. S., J. A. Ericksen, D. E. Schorran, D. W. Johnson, S. E. Lindberg, and J. S. Coleman, 2004: Application of controlled mesocosms for understanding mercury air-soil-plant exchange. *Environ. Sci. Technol.,* **38,** 6044–6050.

Hammerschmidt, C. R., and W. F. Fitzgerald, 2006: Methylmercury in freshwater fish linked to atmospheric mercury deposition. *Environ. Sci. Technol.,* **40,** 7764–7770.

Hicks, B. B., and M. L. Wesely, 1978: An examination of some micrometeorological methods for measuring dry deposition. U.S. EPA Rep. EPA-600/7-78-116, 29 pp.

Horst, T. W., and J. C. Weil, 1994: How far is enough?: The fetch requirements for micrometeorological measurements of surface fluxes. *J. Atmos. Oceanic Technol.,* **11,** 1018–1025.

Howell, J. F., and L. Mahrt, 1997: Multiresolution flux decomposition. *Bound.-Layer Meteor.,* **83,** 117–137.

Lee, X., 2000: Water vapor density effect on measurements of trace gas mixing ratio and flux with a massflow controller. *J. Geophys. Res.,* **105,** 17 807–17 810.

——, G. Benoit, and X. Hu, 2000: Total gaseous mercury concen-

trations and flux over a coastal saltmarsh vegetation in Connecticut, USA. *Atmos. Environ.,* **34,** 4205–4213.

Lindberg, S. E., and W. J. Stratton, 1998: Atmospheric mercury speciation: Concentrations and behavior of reactive gaseous mercury in ambient air. *Environ. Sci. Technol.,* **32,** 49–57.

——, P. J. Hanson, T. P. Meyers, and K.-H. Kim, 1998: Air/surface exchange of mercury vapor over forests—The need for a reassessment of continental biogenic emissions. *Atmos. Environ.,* **32,** 895–908.

——, W. Dong, and T. Meyers, 2002: Transpiration of gaseous elemental mercury through vegetation in a subtropical wetland in Florida. *Atmos. Environ.,* **36,** 5207–5219.

Olofsson, M., B. Ek-Olausson, E. Ljungstrom, and S. Langer, 2003: Flux of organic compounds from grass measured by relaxed eddy accumulation technique. *J. Environ. Monit.,* **5,** 963–970.

——, J. Sommar, E. Ljugstöm, M. Andersson, and I. Wängberg, 2005: Application of relaxed eddy accumulation technique to quantify Hg0 fluxes over modified soil surfaces. *Water Air Soil Pollut.,* **167,** 331–352.

Pattey, E., R. L. Desjardins, F. Boudreau, and P. Rochette, 1992: Impact of density fluctuations on flux measurements of trace gases: Implications for the relaxed eddy accumulation technique. *Bound.-Layer Meteor.,* **59,** 195–203.

——, ——, H. Westberg, B. Lamb, and T. Zhu, 1999: Measurements of isoprene emissions over a black spruce stand using a tower-based relaxed eddy-accumulation system. *J. Appl. Meteor.,* **38,** 870–877.

Pirrone, N., P. Costa, J. M. Pacyna, and R. Ferra, 2001: Mercury emissions to the atmosphere from natural and anthropogenic sources in the Mediterranean region. *Atmos. Environ.,* **35,** 2997–3006.

Raupach, M. R., 1979: Forest flux-gradient anomalies. *Bound.-Layer Meteor.,* **16,** 467–486.

Seigneur, C., K. Vijayaraghavan, K. Lohman, P. Karamchandani, and C. Scott, 2004: Global source attribution for mercury deposition in the United States. *Environ. Sci. Technol.,* **38,** 555–569.

Stull, R. B., 1988: *An Introduction to Boundary Layer Meteorology*. Kluwer Academic, 666 pp.

Vickers, D., and L. Mahrt, 2003: The cospectral gap and turbulent flux calculations. *J. Atmos. Oceanic Technol.,* **20,** 660–672.

Webb, E. K., G. I. Pearman, and R. Leuning, 1980: Correction of flux measurements for density effects due to heat and water vapor transfer. *Quart. J. Roy. Meteor. Soc.,* **106,** 85–100.

Wilks, D. S., 1995: *Statistical Methods in Atmospheric Sciences: An Introduction.* International Geophysical Series, Vol. 59, Academic Press, 464 pp.

Xi, N., P. Zhong, I. J. Beverland, D. H. Oneill, S. L. Scott, and J. B. Moncrieff, 1996: Design, construction and operation of flux measurement systems using the conditional sampling technique. *Atmos. Environ.,* **30,** 3209–3220.

Zhu, T., E. Pattey, and R. L. Desjardins, 2000: Relaxed eddy-accumulation technique for measuring ammonia volatilization. *Environ. Sci. Technol.,* **34,** 199–203.